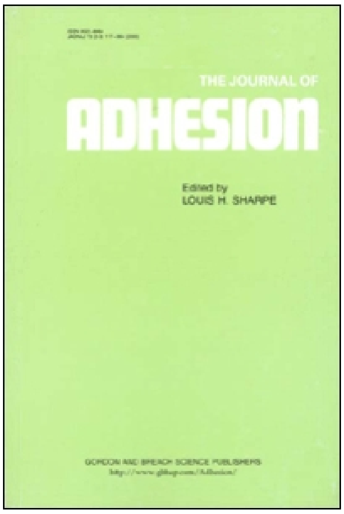

The Journal of Adhesion
Publication details, including instructions for authors and subscription information:
http://www.informaworld.com/smpp/title~content=t713453635

Wettability of Metallic Oxides—Application to Stainless Stell Acid-Base Properties

C. Vittoz[a]; M. Mantel[b]; J. C. Joud[a]
[a] LTPCM-UMR CNRS 5614, INPG Domaine Universitaire, Saint-Martin d'Hères, Cedex, France [b] Centre de Recherche Ugine, Ugine, Cedex, France

To cite this Article Vittoz, C. , Mantel, M. and Joud, J. C.(1998) 'Wettability of Metallic Oxides—Application to Stainless Stell Acid-Base Properties', The Journal of Adhesion, 67: 1, 347 — 358

To link to this Article: DOI: 10.1080/00218469808011116

URL: http://dx.doi.org/10.1080/00218469808011116

J. Adhesion, 1998, Vol. 67, pp. 347–358
Reprints available directly from the publisher
Photocopying permitted by license only

Amsterdam B.V. Published under license
under the Gordon and Breach Science
Publishers imprint.
Printed in India.

Wettability of Metallic Oxides – Application to Stainless Stell Acid-Base Properties

C. VITTOZ [a], M. MANTEL [b] and J. C. JOUD [a,*]

[a]*LTPCM-UMR CNRS 5614, INPG Domaine Universitaire,
BP 75, 38402 Saint-Martin d'Hères Cedex, France;*
[b]*Centre de Recherche Ugine, 73403 Ugine Cedex, France*

(Received 14 May 1997; In final form 7 October 1997)

The Brönsted acid-base properties of oxides of metallic systems are investigated by contact angle measurements of water droplets for different pH. Theoretical analysis based on the electrical and chemical variations of the solid/liquid interfacial tension allows to understand the experimental results observed on model oxide surfaces as SiO_2 and Al_2O_3. Similar wetting measurements are performed on the passive films of a model Fe-Cr-Si alloy and 304 stainless steel. Significant correlations are observed between the contact angle-pH curve and the oxide composition of the passive films deduced from XPS analysis.

Keywords: Contact angle measurements; water; pH; surface tension; interfacial tension; oxide composition; model surfaces; passive film

INTRODUCTION

The work of adhesion, W_{SL}, at a solid-liquid interface could be expressed, following Fowkes' ideas [1], as the sum of two contributions, namely W^{d}_{SL} due to the dispersive or London forces and W^{AB}_{SL} due to non-dispersive or acid-base interactions:

$$W_{SL} = W^{d}_{SL} + W^{AB}_{SL} \tag{1}$$

---

*Corresponding author.

The dispersive component of the work of adhesion, W^{d}_{SL}, can be calculated using the geometric mean relationship:

$$W^{d}_{SL} = 2(\gamma^{d}_{S} \cdot \gamma^{d}_{L})^{1/2} \tag{2}$$

To investigate the Brönsted acid-base contribution, we measure the work of adhesion, W_{SL}, as a function of the pH value of aqueous droplets, following the arguments of Hüttinger *et al.* [2] and Whitesides *et al.* [3]. Such experiments can be performed using contact angle measurements in a one-liquid or a two-liquid configuration [4]. In the last case, the surrounding liquid, H, is a non-polar liquid (alkanes of various chain lengths).

The pH value of the water drop is adjusted with an acid such as HCl or a base such as NaOH or KOH. It has been shown [2] that small amounts of acid or base did not change the surface tension, γ_L, of pure water. Similar results can be obtained for the interfacial tension, γ_{LH} between water (L) and saturated hydrocarbons (H). Experimental results achieved by the pendant drop technique are given in the first part.

In the second part, the work of adhesion of aqueous solutions on model surfaces such as SiO_2 and Al_2O_3 is measured. The observed results are compared with a thermodynamic evaluation of the interfacial tension, γ_{SL}. Taking into account the electrical and chemical contributions of the interfacial tension variations as a function of the pH, we obtain a qualitative evaluation of the p.z.c (pH corresponding to zero charge of the interface). The maximum charge of this interface is also calculated and this value can be, to a first approximation, correlated with the number of Brönsted surface sites of the solid.

As an application of these results, we present in the third part the work of adhesion of aqueous solutions measured on stainless steel surfaces.

PRELIMINARY EXPERIMENTS

Surface Tension Measurements of Aqueous Solutions with Different pH

In a classic one-liquid wetting technique, the basic relationship between the work of adhesion and the contact angle, θ_1, is deduced from Dupré and Young equations (Fig. 1a):

$$W_{SL} = (\gamma_S - \gamma_{SV}) + \gamma_{LV}(1 + \cos\theta_1) \qquad (3)$$

with $\gamma_S - \gamma_{SV} = \pi_e$ the spreading pressure and γ_{LV} the surface tension of the aqueous solution in equilibrium with the vapour phase.

In the two-liquid wetting technique, the same basic relationship between W_{SL} and the contact angle, θ_2, is written (Fig. 1b):

$$W_{SL} = (\gamma_S - \gamma_{SH}) + (\gamma_L - \gamma_{LH}) + \gamma_{LH}(1 + \cos\theta_2) \qquad (4)$$

where $\gamma_{LH}(\gamma_{SH})$ is the interfacial tension between the liquid hydrocarbon, H, and the aqueous solution (the solid surface).

Table I shows surface tension measurements of various aqueous solutions obtained by additions of HCl or NaOH in deionised water. Experimental values are deduced from the pendant drop technique. We can see a slight scatter in the γ_{LV} values but the arithmetic mean value (73.1 mJ· m^{-2}) is nearly identical to the surface tension value of pure water.

Similar results are obtained for the interfacial tension, γ_{LH}. In this case, the alkane, H, is *n*-heptane and the surface tension measurements are performed after an equilibrium time of 1/2 h.

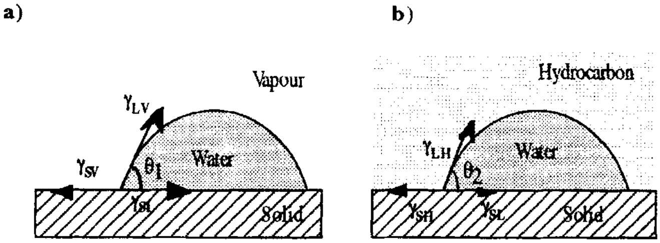

FIGURE 1 a: A one-liquid configuration, b: a two-liquid configuration.

TABLE I Surface tension values of the aqueous test solutions (20°C ± 2)

pH (NaOH/HCl)	*2.9*	*5.1*	*11.1*	*12*
γ_{LV} mJ·m^{-2}	72.9 ± 0.2	73.0 ± 0.3	73.3 ± 0.6	73.2 ± 0.4
γ_{LH} mJ·m^{-2}	52.4 ± 1.5	51.8 ± 1.0	50.2 ± 1.5	51.3 ± 1.3

From these results, and in agreement with the literature [2], a simple pH dependence of W_{SL} can be deduced from Eq. (3) and Eq. (4):

$$\frac{dW_{SL}}{dpH} = -\gamma_{LV} \sin\theta_1 \cdot \frac{d\theta_1}{dpH} \tag{5a}$$

$$= -\gamma_{LH} \sin\theta_2 \frac{d\theta_2}{dpH} \tag{5b}$$

Similarly, using the Dupré expression for the work of adhesion, we obtain a simple dependence of the interfacial tension, γ_{SL}, with the pH:

$$\frac{dW_{SL}}{dpH} = -\frac{d\gamma_{SL}}{dpH} \tag{6}$$

INTERFACIAL TENSION γ_{SL} OF AN OXIDE SURFACE WITH AQUEOUS SOLUTIONS

Theoretical Results

The equilibrium between an oxide and an aqueous solution can be schematized, at a microscopic level, by an hydroxide layer, MOH, in equilibrium with, for example, an acid solution, HY [5]. The variation of the interfacial tension, γ_{SL}, is deduced from the Gibbs adsorption equation at constant temperature [6]:

$$d\gamma_{SL} = -\sum_i \Gamma_i \cdot d\bar{\mu}_i \tag{7}$$

Γ_i is the Gibbs adsorption of the i constituent and $\bar{\mu}_i$ the electrochemical potential.

The application of the equation to the schematized interface leads to a generalization of the Lippmann equation [6]. This relationship, as proposed by Stol and de Bruyn [7] in a slightly different situation, admits an electrical contribution and a chemical contribution to the interfacial tension decrease:

$$d\gamma_{SL} = -\sigma\, d\phi - 2\frac{\sigma}{f} \cdot RT \cdot d \ln|H^+| \tag{8}$$

with σ the surface charge (opposite to the diffuse charge σ_d), ϕ the surface potential, f the Faraday constant ($= N_{AV} \cdot e$ with e the charge of the electron) and $|H^+|$ the proton concentration of the acid solution of concentration C.

Equation (8) can be integrated, using the Graham relationship, to express the diffuse layer charge in a simple Gouy-Chapman interface model [8]. The Graham expression can be written for a 1:1 acid such as HCl or HNO_3 in the S.I. system:

$$\sigma = -\sigma d = (8 \cdot \varepsilon_0 \cdot \varepsilon \cdot \mathrm{RTC})^{1/2} \sinh(f\phi/2\mathrm{RT}) \tag{9}$$

ε is the relative dielectric constant of the solution with concentration C; ε_0 is the dielectric constant of the vacuum.

Taking as an integration constant the interfacial tension γ^0_{SL}, which characterizes the p.z.c., we obtain a general relationship giving the evolution of the interfacial tension, γ_{SL}, with respect to γ^0_{SL}, the surface potential, ϕ, and the surface charge, σ.

$$\gamma_{SL} - \gamma^0_{SL} = -8.\mathrm{C.RT}.\frac{1}{2K}.\left(\frac{f.\phi}{2\mathrm{RT}}\right)^2 + 2.\frac{\sigma_m}{f}.\mathrm{RT}.\ln\left\{1 - \left(\frac{\sigma}{\sigma_m}\right)^2\right\} \tag{10}$$

with $1/K$ as the Debye screening length and σ_m as the maximal surface charge.

Two limiting situations can be easily discussed.

i) When the pH is close to the p.z.c. (*i.e.* $\sigma \ll \sigma_m$), a first order calculation in terms of concentration C gives a parabolic evolution of $\Delta\gamma_{SL}$ with respect to (p.z.c. -pH):

$$\Delta\gamma_{SL} = -4\mathrm{C}.\frac{\mathrm{RT}}{K}(\mathrm{p.z.c.} - \mathrm{pH})^2 \tag{11}$$

ii) When the surface charge, σ, is close to the maximum value, σ_m, the surface potential becomes constant and the interfacial tension variation is linear with respect to the pH variation:

$$\Delta\gamma_{SL}/\Delta\mathrm{pH} = 2.3\mathrm{RT} \cdot 2\sigma_m/f \tag{12}$$

Figure 2 summarizes the previous results. On both sides of the p.z.c, we observe an interfacial tension decrease which is specific of an inversion of the surface charge [5].

Experimental Verifications

Application of such a model is presented on Figure 3 and Figure 4 for an SiO_2 oxide surface and an Al_2O_3 surface, respectively.

Contact angle measurements were performed using a Krüss goniometer in a two-liquid configuration. For each oxide, the pH range of wetting solutions is chosen following corrosion studies and Pourbaix diagrams [9]. For each aqueous solution, the pH value is checked before and after measurements. About 12 sessile drops were

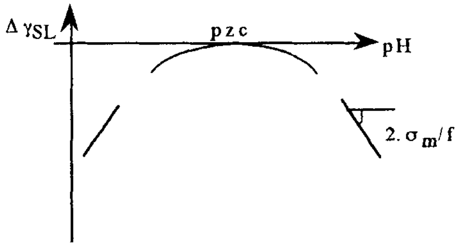

FIGURE 2 Theoretical evaluation of the variation of γ_{SL} with pH of aqueous solutions.

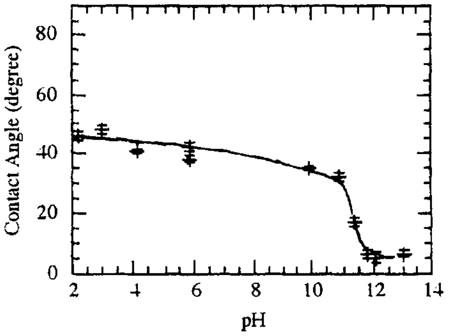

FIGURE 3 Contact angle variations with pH for SiO_2 oxide surface – two-liquid method with octane.

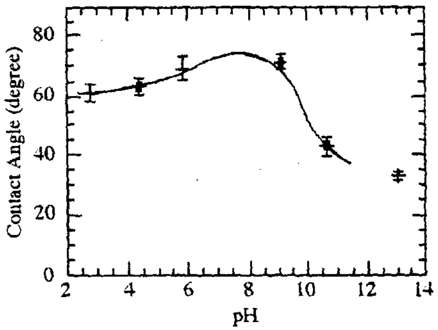

FIGURE 4 Contact angle variations with pH for Al_2O_3 oxide surface – two-liquid method with octane.

put down on the solid substrate; the right and left angles were measured. The tested surfaces were cleaned with acetone and dried with neutral air following a classical procedure. XPS analysis was used to control the cleanliness and the chemical composition of the surface.

For the SiO_2 oxide surface (thermal oxidation of a silicon single crystal), we observe a p.z.c. value close to 2 and a negative surface charge for the whole pH range in agreement with the acid character of SiO_2. The maximum charge, σ_m, can be calculated using Eq. (5b), (6) and Eq. (12) at the inflexion point near pH $\approx$ 11. On the presented experiments, the calculated value is $\sigma_m = -8.4\ \mu C/cm^2$.

The measured values of the wetting angles on the Al_2O_3 oxide surface (sapphire) are characteristic of an amphoteric oxide with a p.z.c. value close to 8. For this analysis, we do not take into account the experimental point at pH = 13 which can be, considering a corrosion aspect, open to criticism.

The observed evolutions are representative of the variations of the work of adhesion, W_{SL}, with the pH of aqueous solutions. Moreover, assuming a constant value with pH for the dispersive part of the work of adhesion, the following condition can be obtained:

$$\frac{dW_{SL}}{dpH} = \frac{dW_{SL}^{AB}}{dpH} \tag{13}$$

This last assumption, in agreement with the literature [2], has been checked by contact angle experiments of the tested aqueous solutions on Teflon® and by two-liquid experiments on SiO_2 following the analysis proposed by Schultz [4]. These results are presented elsewhere.

APPLICATION TO THE CHARACTERIZATION OF THE SURFACE ACID-BASE PROPERTIES OF STAINLESS STEEL

The same experimental analysis is applied to the surface characterization of model alloys Fe-Cr (18.8 at%)-Si (2.3 at%) and a 304 stainless steel (18.5 at% Cr, 8 at% Ni, 0.95 at% Si, bal. Fe).

The FeCrSi Model Alloy

The passive film of the model alloy is obtained by annealing the sample at 820°C during 15 minutes under an H_2/H_2O atmosphere; two different water contents, characterized by two dewpoints, namely (−56°C) and (−58°C) [10], are chosen. A cleaning surface treatment is then carried out in an argon plasma chamber (50 W−10 minutes). As previously measured [11], this cleaning technique fixes a low level of carbon contamination which can be evaluated by XPS analysis, after a few minutes in air, to 2−3 carbon monolayers.

For both annealing treatments, the passive films are characterized by XPS spectra (Fig. 5). Considering only the oxide contributions, the composition of the passive films is estimated using a standard calculation based on the sensitivity factors. The iron, which is only in the metallic form, is assumed to be located below the passive film. The results (Tab. II) clearly show that the composition of the passive films depends strongly on the annealing atmosphere. Indeed, for the sample annealed under the less oxidizing atmosphere (− 58°C) the silicon oxide is the main component of the surface whereas, for the more oxidized sample (−56°C), the amount of chromium oxide in the passive film is more important. In particular in this case, variable angle analysis points out a chromium oxide enrichment at the surface.

For both annealed samples, the wetting results obtained with the two-liquid method (heptane) are presented in Figure 6. We can observe a significant evolution of the contact angle-pH curve with the annealing atmosphere. The evolution obtained on the −58°C sample is

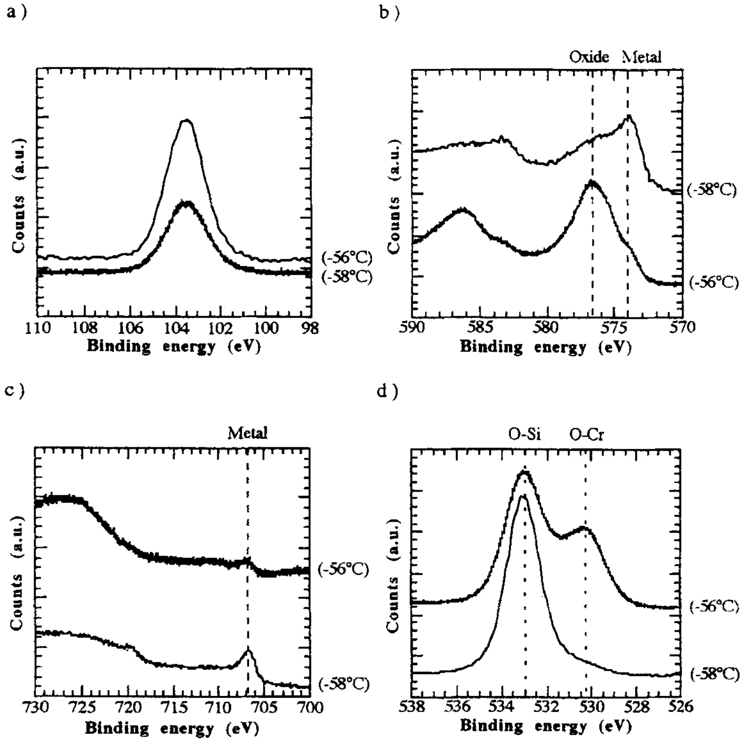

FIGURE 5 XPS spectra of model Fe-Cr-Si alloys exposed to atmospheres with dew point of −58°C and −56°C: a) Si 2p peak, b) Cr 2p peak, c) Fe 2p peak, d) O 1s peak.

TABLE II Surface composition of the passive film of the model Fe-Cr-Si alloy with respect to the annealing atmosphere

Dew point	*Composition of the passive film*						*Surface contamination in carbon (nm)*
	α = 90°			*α = 30°*			
	% Cr^{3+}	% Si^{4+}	% 0	% Cr^{3+}	% Si^{4+}	% 0	
−58°C	1	33	66	1	34	65	0.2
−56°C	11	21	68	11	15	74	0.3

roughly comparable with the evolution of the conact angle-pH curve achieved on thermally-grown silicon oxide. On the contrary, the curve obtained on the −56°C sample exhibits two humps, the first centered around pH ≈ 2.5 and the second around pH ≈ 7, which are character-

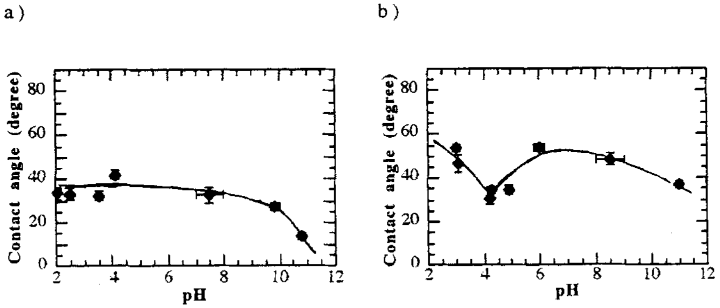

FIGURE 6 Contact angle variations with pH for Fe-Cr-Si model alloys a: dew point −58°C, b: dew point −56°C (two-liquid method with heptane).

istic of the p.z.c. values of silicon oxide and chromium oxide, [12] respectively.

The 304 Stainless Steel

The 304 stainless stell suffers an industrial thermal treatment under H_2 atmosphere to obtain a passive film [13]. Plasma-cleaned surfaces were characterized by XPS. The analysis indicates the presence in the film of chromium, silicon and a significant amount of iron in the form of oxides and/or hydroxides. Angular analysis shows a chromium depletion and an hydroxide enrichment at the surface (Fig. 7,

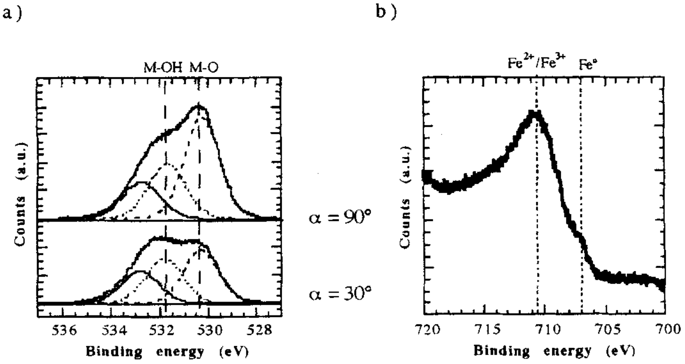

FIGURE 7 XPS spectra of 304 stainless steel: a) O 1s peak for two analysis angles – M stands for Cr and Fe-, b) Fe $2p_{3/2}$ peak.

Tab. III). In other words, these results seem to indicate that the silicon oxide and the iron hydroxide are more particularly located at the outer part of the passive film.

The wetting results obtained on the 304 stainless steel are indicated in Figure 8. The contact angle evolution with respect to the pH values can be, in a first analysis, viewed as an acid surface (dotted curve in Fig. 8). We observe, indeed, at high pH values, a significant decrease of the contact angles which indicates the existence of negative surface charges. From the presented data, the maximum surface charge calculated at the inflexion point (pH $\cong$ 10.3) is $\sigma_m \simeq -13$ $\mu C/cm^2$. However, a more detailed examination of the experimental points allows one to note the premise of two humps centered on the pH values 2 and 9 which can be related, in agreement with XPS analysis, to the p.z.c. values of silicon oxide and iron hydroxides, respectively [12].

CONCLUSION

Measuring the contact angle of a water drop at different pH is a possible way to obtain information on the acid-base properties of the

TABLE III Surface composition of the passive film of 304 stainless steel

Analysis angle	*at.% O*	*Composition of the passive film* *at.% Cr(ox)*	*at.% Fe(ox)*	*at.% Si(ox)*
$\alpha = 90°$	73	7	15	5
$\alpha = 30°$	77	2	13	8

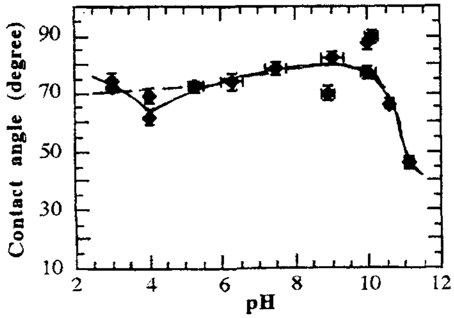

FIGURE 8 Contact angle variations with pH for the passive layer of a 304 stainless steel (two-liquid method with heptane).

oxide surface of a metallic system. Taking into account the electrical and chemical contributions of the interfacial tension variations as a function of the pH, a qualitative evaluation of the p.z.c. is obtained and the maximum charge of the interface is calculated. This analysis has been done with success on model surfaces such as SiO_2 and Al_2O_3. Contact angle measurements were also performed on model Fe-Cr-Si alloys and 304 stainless steel which exhibit a passive film obtained by thermal treatment. Concerning Fe-Cr-Si alloys, a strong correlation between the chemical composition of the passive film and the contact angle-pH curve is observed. In particular, for the sample exposed to the atmosphere with a dew point of −56°C, the two maxima observed on the pH curve can be associated with the existence of silicon oxide and chromium oxide in the passive film as indicated by XPS analysis. The wetting results obtained on the 304 stainless steel are typical of classic acid surface behaviour. Nevertheless, we can find again an amazing correlation between XPS analysis and contact angle-pH curve.

References

[1] Fowkes, F. M., *in Acid Base Interactions*, Mittal, K. L. and Anderson, H. R. Eds. (V. S. P., Zeist, 1991). p. 93.
[2] Hüttinger, K. J., Höhmann-Wien, S. and Krekel, G., *J. Adhesion Sci. Technol.* **6**, 317 (1992).
[3] Whitesides, G. M. and Laibinis, P. E., *Langmuir* **6**, 87 (1990).
[4] Schultz, J., Tsutsumi, K. and Donnet, J. P., *J. Colloid Interface Sci.* **59**, 272 (1977).
[5] Jolivet, J. P., *De la solution à l'oxyde* (Inter-Editions & CNRS Editions, Paris, 1994).
[6] Defay, R. and Prigogine, I., *Surface Tension and Adsorption* (Longmans, London, 1996).
[7] Stol, R. and de Bruyn, P. L., *J. Colloid Interface Sci.* **75**, 185 (1980).
[8] Bockris, J. and Reddy, A. K., *Modern Electrochemistry 2* (Plenum Press, N.Y., 1977).
[9] Pourbaix, M., *Atlas d'équilibres electrochimiques* (Gauthiers-Villars, Paris, 1963).
[10] Gorse, D., Joud, J. C. and Baroux, B., *Corrosion Science* **33**, 1455 (1992).
[11] Mantel, M. and Wightman, J. P., *Surf. Interf. Analysis* **21**, 595 (1994).
[12] Parks, G. A., *Chem. Rev.* **65**, 177 (1965).
[13] Lacombe, P., Baroux, B. and Béranger, G., *Les Aciers Inoxydables* (Les Editions de Physique Les Ulis, 1990).